*Int. J. Cancer:* **123,** 2267–2278 (2008)


# Tumor expressed PTHrP facilitates prostate cancer-induced osteoblastic lesions

**Jinhui Liao[1], Xin Li[1], Amy J. Koh[1], Janice E. Berry[1], Nanda Thudi[2], Thomas J. Rosol[2], Kenneth J. Pienta[3,4] and Laurie K. McCauley[1,5]***

[1]*Department of Periodontics and Oral Medicine, School of Dentistry, University of Michigan, Ann Arbor, MI*
[2]*Department of Veterinary Biosciences, College of Veterinary Medicine, Ohio State University, Columbus, OH*
[3]*Department of Urology, Urology Center, University of Michigan, Ann Arbor, MI*
[4]*Department of Internal Medicine, University of Michigan, Ann Arbor, MI*
[5]*Department of Pathology, Medical School, University of Michigan, Ann Arbor, MI*

**Expression of parathyroid hormone-related protein (PTHrP) correlates with prostate cancer skeletal progression; however, the impact of prostate cancer-derived PTHrP on the microenvironment and osteoblastic lesions in skeletal metastasis has not been completely elucidated. In this study, PTHrP overexpressing prostate cancer clones were stably established by transfection of full length rat PTHrP cDNA. Expression and secretion of PTHrP were verified by western blotting and IRMA assay. PTHrP overexpressing prostate cancer cells had higher growth rates *in vitro*, and generated larger tumors when inoculated subcutaneously into athymic mice. The impact of tumor-derived PTHrP on bone was investigated using a vossicle co-implant model. Histology revealed increased bone mass adjacent to PTHrP overexpressing tumor foci, with increased osteoblastogenesis, osteoclastogenesis and angiogenesis. *In vitro* analysis demonstrated pro-osteoclastic and pro-osteoblastic effects of PTHrP. PTHrP enhanced proliferation of bone marrow stromal cells and early osteoblast differentiation. PTHrP exerted a pro-angiogenic effect indirectly, as it increased angiogenesis but only in the presence of bone marrow stromal cells. These data suggest PTHrP plays a role in tumorigenesis in prostate cancer, and that PTHrP is a key mediator for communication and interactions between prostate cancer and the bone microenvironment. Prostate cancer-derived PTHrP is actively involved in osteoblastic skeletal progression.**


**Key words:** parathyroid hormone-related protein; PTHrP; skeletal metastasis; prostate carcinoma; angiogenesis

Prostate cancer is a common malignant disease that characteristically affects bones as it progresses. More than 65–75% of late stage patients have skeletal metastases.[1] The progression of prostate cancer in bone results in pathological fractures, bone pain and spinal cord compression. These complications severely lower patients' quality of life.[2,3] Prostate cancer skeletal involvement is a complicated process, in which bone provides a favorable medium for tumor growth, resulting in alterations in bone remodeling and development of cancer-associated bone lesions. Prostate cancer and the bone microenvironment communicate and interact with each other throughout the progression of skeletal metastasis.

Clinical studies have shown that prostate cancer metastases are often in the axial skeleton and long bone metaphyses, sites with active remodeling.[4,5] *In vivo* studies in animal models support the hypothesis that prostate cancers prefer to localize at regions with high bone turnover.[6,7] Studies have shown that enhancing bone turnover increased the localization of prostate cancer to the skeleton, whereas inhibiting bone resorption suppressed skeletal lesions by prostate cancer cells.[8–10] Prostate cancer cells may, like hematopoietic stem cells, adhere and localize at active remodeling sites by a calcium sensing receptor-mediated mechanism, at least in part, regulated by the action of parathyroid hormone-related protein (PTHrP).[11–13]

High expression of PTHrP correlates with skeletal metastasis in numerous cancers including prostate cancer.[14] Expression of PTHrP in prostate cancer has been associated with increased malignancy.[15] It has been proposed that tumor-derived PTHrP plays a critical role in skeletal metastasis by a vicious cycle, in which PTHrP enhances bone remodeling and release of numerous biological factors, providing a fertile environment for further tumor growth.[2] Tumor-derived PTHrP may also facilitate skeletal progression by directly stimulating tumor cell proliferation, adhesion and survival using autocrine or paracrine mechanisms.[16–21]

Tumor-derived PTHrP may be an important mediator of cancer-induced skeletal lesions. PTHrP has some of the same biological effects as PTH by binding to their common receptor, the PTHR1. Both can have dual effects on bone remodeling. It has been well characterized that PTH and PTHrP are potent stimulators of osteoclastogenesis by enhancing the production of RANK ligand (RANKL) and MCP-1 by osteoblasts.[22,23] RANKL induces differentiation of osteoclast progenitor cells, and results in increased bone resorption. However, PTH and PTHrP also have anabolic effects on bone through mechanisms that are not yet well characterized.[24]

Unlike other skeletal metastases which are typically osteolytic, most prostate cancers result in osteoblastic skeletal lesions,[3] characterized as increased bone formation. Several osteoblastic factors, such as BMPs, TGF-β, FGFs, IGFs, PDGF, VEGF and endothelins, are produced by prostate cancer cells. Most of these factors regulate osteoblast function by activating signaling pathways involved in osteoblast proliferation and differentiation.[25] VEGF may exert an osteoblastic role indirectly by promoting angiogenesis.[26] Recently, it has been reported that Wnt signaling may be one of the switches that converts prostate cancer bone metastatic activity from osteolytic to osteoblastic.[27]

In this study, it was hypothesized that prostate cancer-derived PTHrP is an important factor that mediates interactions between the bone marrow microenvironment and prostate cancer, which further facilitates the establishment of skeletal metastases and osteoblastic alterations.

---

Additional Supporting Information may be found in the online version of this article.

*Abbreviations:* ALP, alkaline phosphatase; BMSC, bone marrow stromal cell; CFU-ALP, alkaline phosphatase-positive colony forming units; CFU-F, fibroblast colony forming units; GAPDH, glyceraldehyde 3-phosphate dehydrogenase; HAEC, human aortic endothelial cells; HBME, human bone marrow endothelial cells; IRMA, Immunoradiometric assay; PCa, prostate carcinoma; PCR, polymerase chain reaction; PTH, parathyroid hormone; PTHrP, parathyroid hormone-related protein; PTHR1, PTH/PTHrP receptor 1; RANK, receptor activator of NF-kB; RANKL, receptor activator of NF-kB ligand; TRAP, tartrate-resistant acid phosphatase; vWF, von Willebrand factor.

Grant sponsor: National Cancer Institute; Grant number: P01-CA093900.

***Correspondence to:** Department of Periodontics and Oral Medicine, University of Michigan School of Dentistry, 1011 N. University Ave., Ann Arbor, MI 48109-1078, USA. E-mail: mccauley@umich.edu

Received 31 August 2007; Accepted after revision 20 February 2008
DOI 10.1002/ijc.23602
Published online 26 August 2008 in Wiley InterScience (www.interscience.wiley.com).

## Material and methods

### *Cell lines and tissue culture*

The ACE-1 canine prostate cancer cell line[28] was maintained at 37°C and 5% $CO_2$ in RPMI 1640 containing 10% fetal bovine serum (FBS) and 1% penicillin–streptomycin (Invitrogen Corp., Carlsbad, CA). Human aorta endothelial cells (HAEC) and human bone marrow endothelial cells (HBME) were maintained in DMEM medium containing 10% FBS and 1% penicillin–streptomycin.

### *Reagents*

LipofectAMINE Plus lipid based transfection reagent was obtained from Invitrogen. PTHrP peptide (1–34) and PTHrP (7–34) were obtained from Bachem California (Torrance, CA). CHAPS (3-[(3-cholamidopropyl)dimethylammonio]-1-propanesulfonic acid) was from U.S. Biochemical Corp. (Cleveland, OH). Rabbit anti-von Willebrand factor (vWF) antibody was acquired from NeoMarkers (Fremont, CA). Anti-PTHrP rabbit antibody for immunohistostaining was from EMD Biosciences (San Diego, CA). Anti-PTHrP rabbit antibody for Western blot was from Santa Cruz Biotechnology (Santa Cruz, CA). Anti-Ki67 was obtained from Abcam (Cambridge, MA). Dexamethasone, mouse anti-tubulin antibody and bovine serum albumin were obtained from Sigma Aldrich (St. Louis, MO).

### *Transfection and selection*

A full-length rat PTHrP cDNA (1–141) was cloned into expression vector pcDNA3 (Invitrogen).[29] The pcDNA3.1+ control vector was obtained from Invitrogen. All transfections were performed with LipofectAMINE Plus reagents following manufacturer's recommended protocols. After transfection, resistant clones were selected with 800 μg/ml G418. The expression of target genes was screened by Western blot analysis. The secreted PTHrP was analyzed using an IRMA system (Diagnostic Systems Laboratories, Inc., Webster, Texas) according to manufacturer's direction.

### *Western blot analysis*

Cells were washed in ice-cold 1× PBS, scraped, and pelleted by centrifugation (500*g*, 5 min). The cell pellet was resuspended and incubated for 15 min in 1× lysis buffer [20 mmol/l MOPS, 5 mmol/l $MgCl_2$, 0.1 mmol/l ethylene-diamine-tetra-acetic acid (EDTA), 200 mmol/l sucrose (pH 7.4), containing 1% CHAPS and phosphatase and protease inhibitors]. Cell suspensions were centrifuged at 13,000*g* for 10 min to remove nuclei and cell debris. The protein concentration was determined by Bradford method. Lysates containing equal amounts of protein (50 μg) were separated by SDS-PAGE and transferred to polyvinylidene difluoride membrane (Bio-Rad Laboratories, Hercules, CA). The membrane was blocked with 5% nonfat milk in TBS-0.1% Tween 20. Blots were incubated with primary antibodies for 2 hr at room temperature or overnight at 4°C. Following washing in TBS-0.1% Tween 20, blots were incubated with horseradish peroxidase-labeled secondary antibodies (1:10,000) for 1 hr at room temperature. After washing, the signals were detected by standard enhanced chemiluminescence.

### *Growth curve* in vitro

Five thousand ($5 \times 10^3$) cells were plated in each well of 24-well plates in quadruplicate in the presence of serum at indicated concentrations. The cells were fixed on the indicated days for subsequent staining with crystal violet.[30] DNA binding dye was solubilized with 10% acetic acid. Relative cell numbers were measured by optical density at 595 nm.

### *Experimental animals*

All experimental animal procedures were performed in compliance with the institutional ethical requirements and were approved by the University of Michigan Committee for the Use and Care of Animals. Athymic mice (4–6 weeks) were purchased from Harlan, (Indianapolis, IN). (*i*) Male athymic mice (5 animals per condition in 2 separate experiments) were injected subcutaneously in each flank with $5 \times 10^4$ tumor cells, which were suspended at $5 \times 10^6$ cells/ml in Hank's buffered saline solution (Invitrogen). After 6 weeks, tumors were dissected and weighed. (*ii*) Bone implantation was performed as previously described, with minor modification.[31] Briefly, vertebrae were isolated under sterile condition from 8-day old mice. Soft tissue was dissected, and vertebrae were sectioned into vertebral bodies (vossicles) with a scalpel blade. Five thousand ($5 \times 10^3$) prostate cancer cells were injected into each vossicle. Male athymic mice were used as transplant recipients (5 animals per condition in 2 separate experiments). After anesthesia (i.p. injection of a mixture of ketamine [90 mg/kg] and xylazine [5 mg/kg]), vossicles (4 per mouse) were implanted into subcutaneous pouches. One centimeter incisions were made along the backs of mice, pouches were made on either side of the incision with blunt dissection, and vossicles were implanted. After 6 weeks, vossicles were removed from transplant recipients, and exposed to X-ray film (Wolverine X-Ray, Dearborn, MI) at 3×, 32 kV, 45 sec in a microradiography X-ray machine (Faxitron, Madison, WI) to compare bone density.

### *Histomorphometry and Immunohistochemistry*

All samples were fixed with PBS-buffered 10% (v/v) formaldehyde for 24 hr. Bone samples were demineralized in 10% EDTA (pH 7.4) for 4 weeks. Tissues were paraffin embedded, sectioned and stained with either hematoxylin and eosin (H&E), Trichrome stain for bone, TRAP staining for osteoclasts, or used for immunohistochemistry. For immunohistochemistry, tissue sections were deparaffinized with xylene and rehydrated through a series of graded ethanol (100, 95, 70, 50 and 30%), with a final wash in water. Antigen retrieval was performed with 5 mg/ml pepsin in 5 mM HCl at 37°C for 10–15 min. Standard indirect immunoperoxidase procedures were used for immunohistochemistry using the AEC system Cell and Tissue staining kit (R&D systems, Minneapolis, MN). Mayer's hematoxylin (Sigma-Aldrich, Sigma, St. Louis, MO) was used for counterstaining. The proliferation marker Ki-67 index was determined by the average percentage of tumor cells with nuclear staining in 5 different 400× fields.

### *Microvessel density analysis*

Microvessel density analysis (MVD) was performed as described in the literature[32] with modification. Tissue sections were stained for vWF using immunohistochemistry. Four random areas per tumor section were selected. Any single or cluster of endothelial cells that was clearly separated from adjacent microvessels was considered as one countable microvessel. The average vessel count (MVD) was determined for each specimen. For tissue array, total numbers of vessels were used as MVD for each individual section.

### *Colony formation assay*

Bone marrow cells were isolated from long bones as previously described.[33] Briefly, bone marrow from the femoral, tibial and humeral cavities was flushed using α-modified minimum essential medium (α-MEM) with 20% serum and 10 nM dexamethasone.

CFU assays were performed as described[34] with modification. Bone marrow cells ($5 \times 10^6$) were plated onto 6-well culture plates in α-MEM with 20% serum, 10 nM dexamethasone, 50 μg/ml ascorbic acid and 10 mM β-glycerophosphate containing either vehicle or indicated concentrations of PTHrP (1–34). Vehicle or PTHrP (1–100 nM) was added to cultures every other day. After 10 days, colonies formed were fixed and stained for alkaline phosphatase activity (ALP) to detect positive colonies (CFU-ALP), followed by crystal violet stain for total colonies (CFU-F). The staining of ALP activity *in situ* was performed with a histochemical kit from Sigma following manufacturer's procedure.

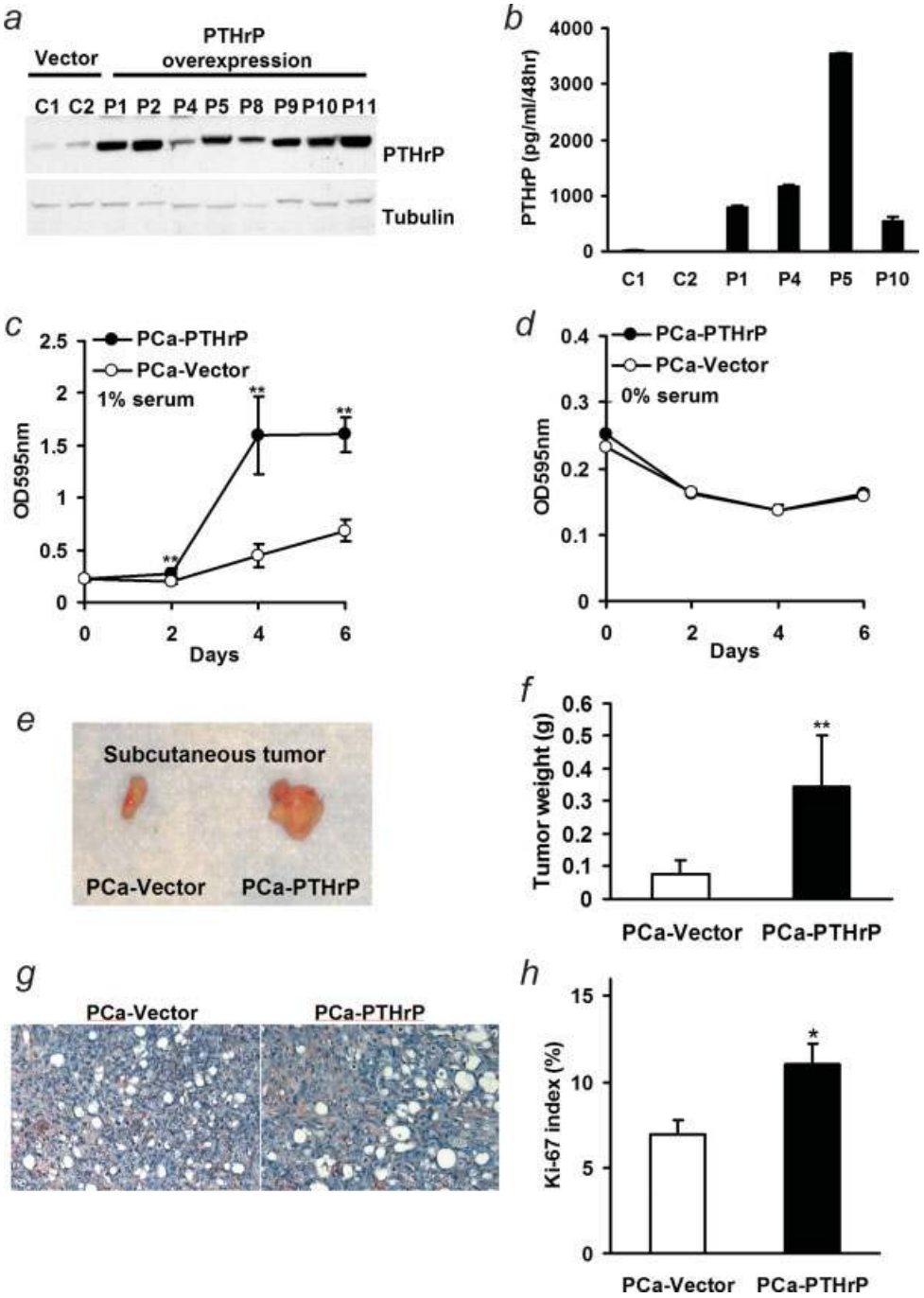


**Figure 1** – Characterization of PTHrP overexpressing ACE-1 cells. (*a*) Full length rat PTHrP cDNA was transfected into the ACE-1 canine prostate cancer cell line using LipofectAMINE Plus. Stable clones were selected with G418. Expression levels of PTHrP in cell lysates were screened with western blot; (*b*) secretion of PTHrP in medium by prostate cancer stable clones was verified with IRMA; (*c*,*d*) comparison of *in vitro* proliferation assay of vector control (PCa-Vector) and PTHrP overexpressing ACE-1 cells (PCa-PTHrP) in the presence of 1% (*c*) and 0% serum (*d*). Cell numbers at indicated days were measured by crystal violet staining and shown as optical density at 595 nm (**$p < 0.01$, PCa-PTHrP *vs*. PCa-Vector, $n = 4$); (*e*) representative images of subcutaneous tumors. (*f*) Subcutaneous growth of PCa-PTHrP tumor and vector control after 6 weeks (**$p < 0.01$, PCa-PTHrP *vs*. PCa-Vector, $n = 5$); (*g*) vWF as a marker of vascularity was determined by immunostaining in sections of subcutaneous tumors. Sections were counterstained with Mayer's hematoxylin. (red, vWF; blue, nuclei; magnification ×200). (*h*) Proliferation rate was measured with immunohistostaining for Ki-67 (*$p < 0.05$, PCa-PTHrP *vs*. PCa-Vector, $n = 8$ and 7, respectively).

In vitro *osteoclastogenesis*

Bone marrow cells ($5 \times 10^6$) were plated onto 6-well culture plates in α-MEM with 20% serum, 10 nM dexamethasone, 50 μg/ml ascorbic acid and 10 mM β-glycerophosphate. After treatment with vehicle, PTHrP (1–100 nM), or conditioned medium every other day for 10 days, cells were fixed, stained for TRAP positive cells (per protocol from the Luckeucyte Acid-phosphatase staining kit (Sigma)), and conterstained with Mayer's hematoxylin. Osteoclast-like cells in each well were scored by counting the number of TRAP-positive cells containing 3 or more nuclei.

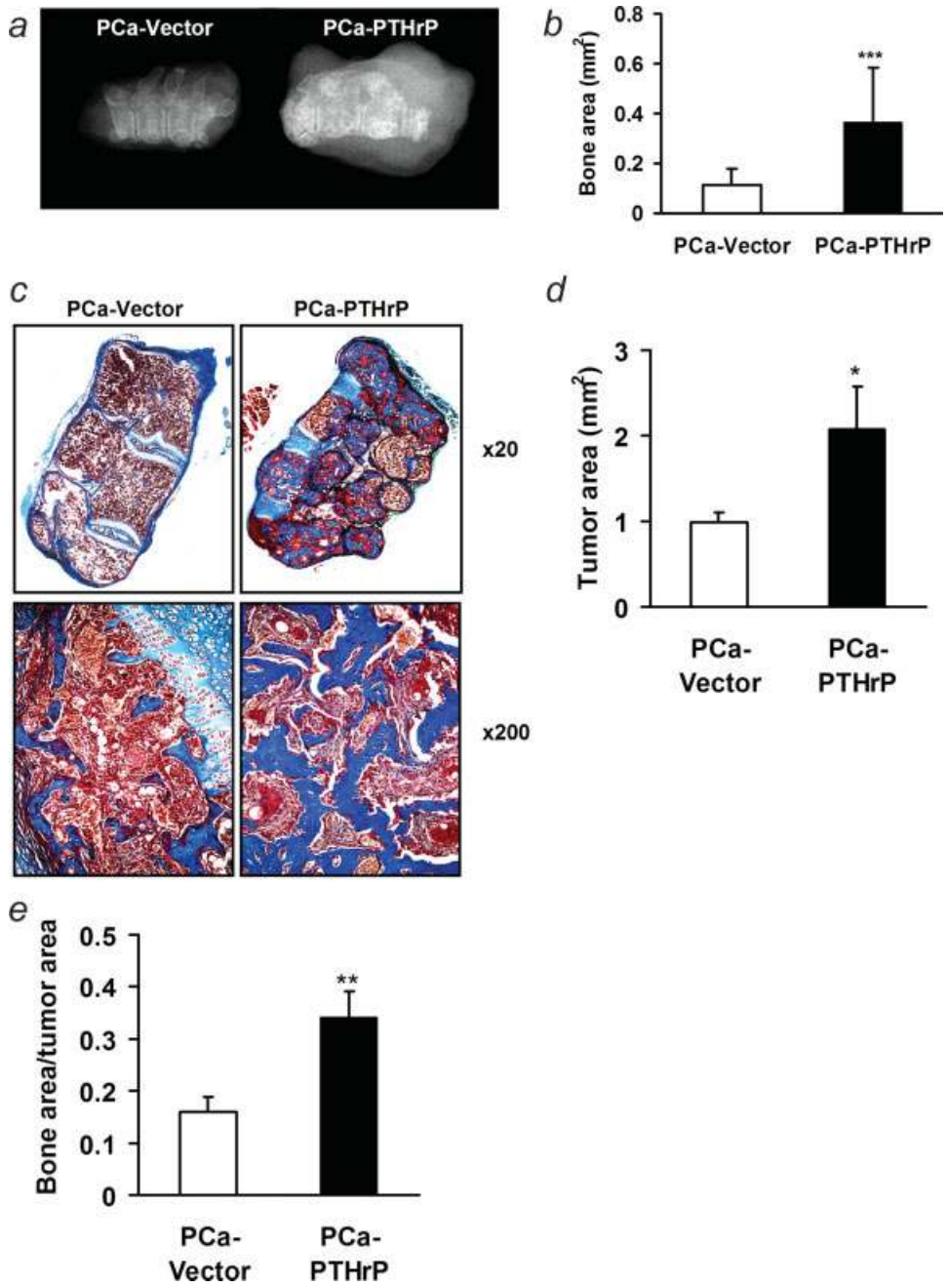


**Figure 2** – Osteoblastic lesions in vossicle implants with PTHrP overexpressing tumors. (*a*) Representative radiography of vossicles; (*b*) quantification of bone area in vossicle implants from trichrome-stained sections (***$p < 0.001$, PCa-PTHrP *vs.* PCa-Vector, $n = 19$ and 20, respectively); (*c*) representative trichrome staining of vossicles with PCa-PTHrP and PCa-Vector (magnification ×20). PTHrP overexpressing tumors resulted in greater bone area (stained in blue) compared to vector controls. (*d*) Quantification of tumor area in vossicle implants from HE-stained sections (*$p < 0.05$, PCa-PTHrP *vs.* PCa-Vector, $n = 19$ and 20, respectively; (*e*) bone area/tumor area (**$p < 0.01$, PCa-PTHrP *vs.* PCa-Vector, $n = 19$ and 20, respectively).

In vitro *osteoblastogenesis*

Freshly isolated bone marrow cells were maintained in α-MEM with 20% serum, and 10 nM dexamethasone at 37°C in an atmosphere of 100% humidity and 5% carbon dioxide. Medium was refreshed after 1 week. The adherent cell layers (bone marrow stromal cells, BMSC) were harvested when confluent. One hundred thousand ($1 \times 10^5$) cells were seeded in each well of a 12-well plate. The medium was refreshed every other day with α-MEM containing 20% serum, and 10 nM dexamethasone, 50 μg/ml ascorbic acid and 10 mM β-glycerophosphate, plus either vehicle or PTHrP (10 nM). One week later, staining for ALP activity was performed as described earlier. The intensity of ALP staining was quantified from scanned plates using a UMAX scanner (Techville, Dallas, TX) and Image pro plus software (Media Cybernetics, Bethesda, MD). For co-culture assays, 2,000 ($2 \times 10^3$) prostate cancer cells were coplated with $1 \times 10^5$ BMSC into 12-well plates in α-MEM with 20% serum, and 10 nM dexamethasone, 50 μg/ml ascorbic acid and 10 mM β-glycerophosphate. Medium was refreshed

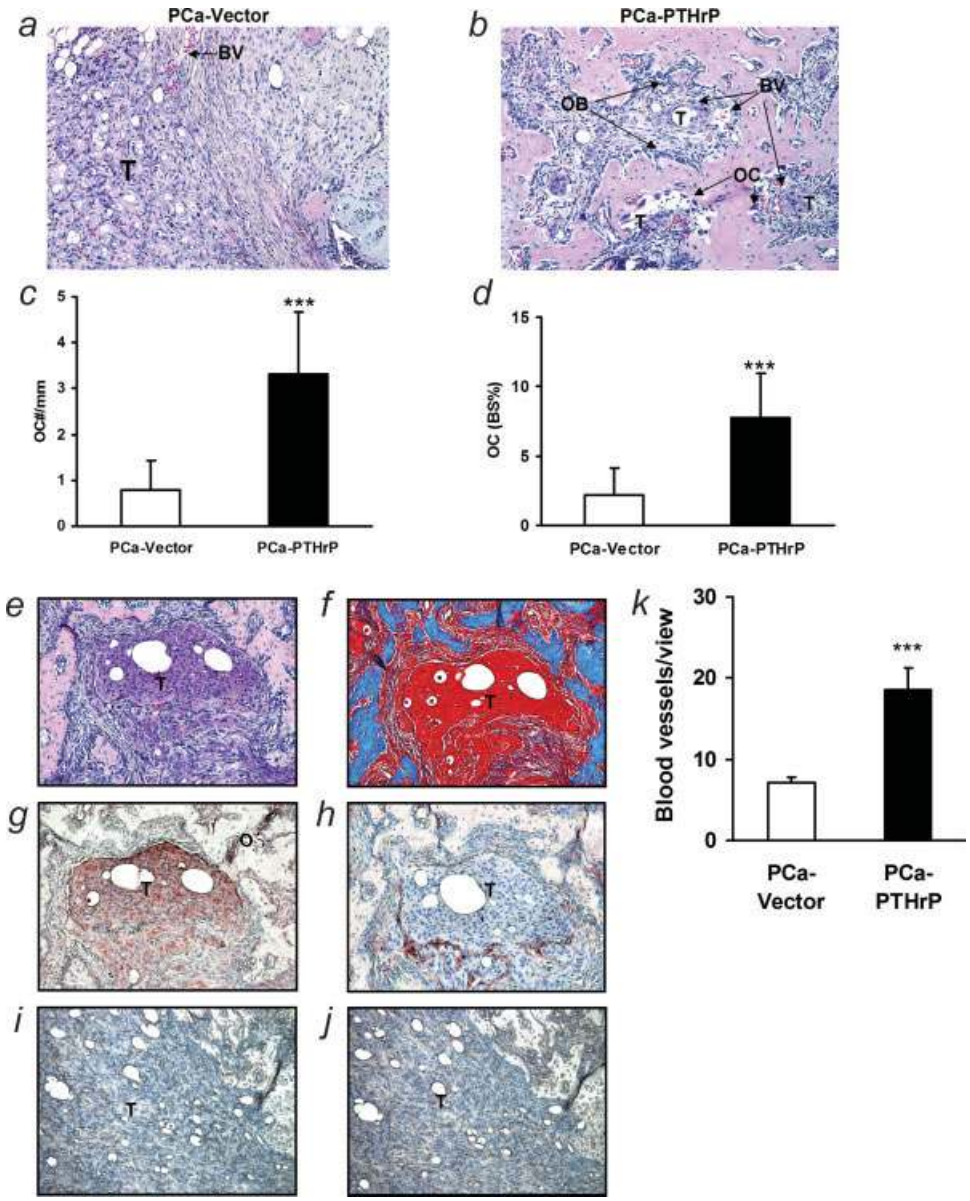


**Figure 3** – Alterations in the microenvironment with tumor-derived PTHrP. (*a,b*) Representative H&E-stained sections (T, tumor; OB, osteoblasts; OC, osteoclasts; BV, blood vessel; magnification ×200); (*c*) quantitative numbers of osteoclasts per mm bone surface (***$p < 0.001$, PCa-PTHrP *vs*. PCa-Vector, $n = 19$ and 15, respectively); (*d*) quantitative data of osteoclasts covering bone surfaces (***$p < 0.001$, PCa-PTHrP *vs*. PCa-Vector, $n = 19$ and 15, respectively); (*e–h*) localization of tumor, bone, and vascularity. Consecutive sections of osteoblastic lesions by PCa-PTHrP were stained with H&E (*e*) and trichrome (*f*; bone: blue), or immunostained for PTHrP (*g*; PTHrP: red) or vWF (*h*; vWF: red) (T, tumor) (magnification ×200). (*i,j*) Consecutive sections of vossicle implant with PCa-vector immunostained for PTHrP (*i*) or vWF (*j*); (*k*) MVD in tumor area was measured using vWF staining. (***$p < 0.001$; PCa-PTHrP *vs*. PCa-Vector, $n = 18$ and 20, respectively).

every other day. After 1 week, ALP staining and quantification were performed as described earlier. The arbitrary relative units were obtained by comparing with vehicle control.

*Endothelial sprout network formation assay*

Growth factor-reduced Matrigel (BD Biosciences, San Jose, CA) was placed in 8-well chamber slides, and incubated at 37°C for 30 min to allow the Matrigel to polymerize.[35] Six thousand ($6 \times 10^3$) HAEC were added to the top of the Matrigel in each well. The chambers were then incubated at 37°C for 24 hr. After incubation, the slides were fixed and stained with Hema 3 STAT PACK (Protocol, Kalamazoo, MI). The slides were examined, and the sprouts were counted under a light microscope. For co-culture assays, equal numbers of BMSC and endothelial cells were included.

*RNA isolation, reverse transcription and real-time PCR*

Total RNAs were prepared using Trizol reagent (Invitrogen). Total RNA (1 μg) was reverse transcribed in a 20 μl reaction volume containing random hexamers with a reverse transcription assay system (Applied Biosystems, Foster City, CA). Reverse transcription was performed at 25°C for 10 min, 48°C for 30 min and 95°C for 5 min. Real-time PCR was performed using the ABI PRISM 7700 with FAM-labeled probe assay system (Applied Biosystems, Foster City, CA). GAPDH was used as an internal control.

*Statistical analysis*

Student's *t*-test for independent analysis was applied to evaluate differences using the GraphPad Instat software program

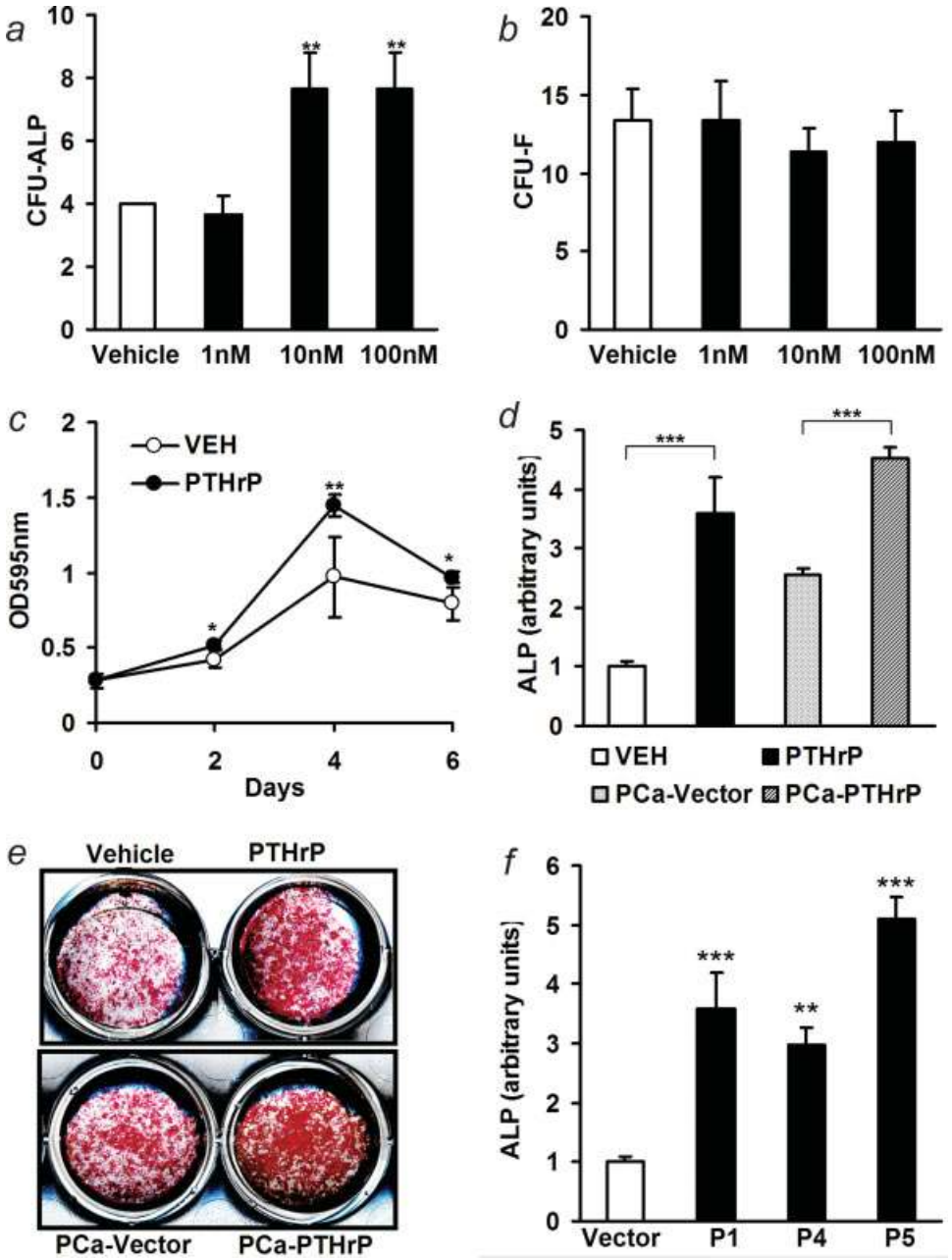


**Figure 4** – PTHrP induced osteoblastogenesis. (*a*,*b*) CFU assay. Bone marrow cells ($5 \times 10^6$) were plated onto 6-well culture plates and were treated with vehicle or PTHrP(1–34) (1–100 nM). CFU-ALP and CFU-F were measured at day 7 (**$p < 0.01$, PTHrP *vs*. vehicle control, $n = 4$ each); (*c*) proliferation of bone marrow stromal cells in response to PTHrP (10 nM), as measured with crystal violet staining (*$p < 0.05$, **$p < 0.01$, PTHrP *vs*. vehicle control, $n = 4$); (*d*) comparative ALP staining *in vitro* was measured as described in materials and methods (***$p < 0.001$, $n = 3$); (*e*) representative ALP staining of BMSC culture with treatment of vehicle or PTHrP (10 nM), or co-cultured with PCa-PTHrP or PCa-Vector for 7 days; (*f*) comparison of pro-osteoblastogenic ability in different clones of PTHrP overexpressing ACE-1 cells with vector control using ALP staining. P1, P4 and P5 secreted low, medium and high levels of PTHrP, respectively (**$p < 0.01$, ***$p < 0.001$, *vs*. vector control, $n = 6$). [Color figure can be viewed in the online issue, which is available at www.interscience.wiley.com.]

(GraphPad Software, San Diego, CA). The value $p < 0.05$ was considered statistically significant. All assays were repeated at least twice with similar results.

## Results

### *Over expression of PTHrP enhanced prostate cancer tumorigenesis*

A full-length rat PTHrP (1–141) cDNA was transfected into ACE-1 prostate cancer cells. PTHrP overexpressing clones stably selected in G418 were screened using Western blotting (Fig. 1*a*), and the secreted PTHrP levels of selected clones were measured with IRMA (Fig. 1*b*). The secreted PTHrP concentrations in vector controls were 2.27–13.21 pg/ml/48 hr, while the PTHrP-overexpressing clones secreted 546–3,543 pg/ml/48 hr. Unless otherwise indicated, PTHrP-overexpressing clone 5 was used for the majority of experiments.

To measure cell numbers over time, cells were cultured for 6 days in medium that contained either 0 or 1% serum. Cell numbers at indicated days were measured by crystal violet staining and are

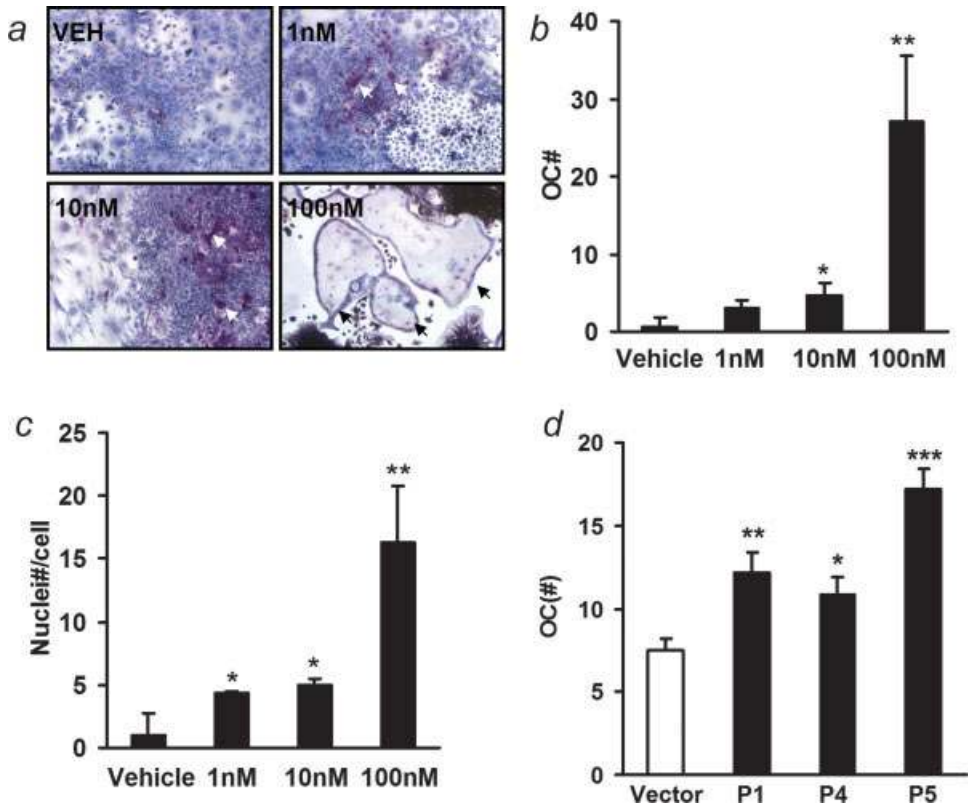


**Figure 5** – PTHrP induced osteoclastogenesis. (*a*) Representative data of *in vitro* osteoclastogenesis by PTHrP from whole bone marrow (magnification ×100). Bone marrow cells ($5 \times 10^6$) were plated into 6-well culture plates and were treated with vehicle or PTHrP (1–100 nM) every other day for 10 days. TRAP staining was performed. Osteoclasts are indicated with arrows; (*b*) the numbers of osteoclasts were counted as TRAP-positive cells with 3 or more nuclei (*$p < 0.05$, **$p < 0.01$, PTHrP *vs.* vehicle, $n = 3$); (*c*) average numbers of nuclei per osteoclast. (*$p < 0.05$, **$p < 0.01$, PTHrP *vs.* vehicle, $n = 3$); (*d*) comparison of pro-osteoclastogenic ability of different clones of PTHrP overexpressing ACE-1 cells with vector control using TRAP staining. P1, P4 and P5 secreted low, medium and high level of PTHrP, respectively (*$p < 0.05$, **$p < 0.01$, ***$p < 0.001$, *vs.* vector control, $n = 3$). [Color figure can be viewed in the online issue, which is available at www.interscience.wiley.com.]

shown as optical density at 595 nm. Prostate cancer cells with PTHrP overexpression had increased growth rate over time in the presence of 1% serum (Fig. 1*c*). Without serum, both PTHrP overexpressing prostate cancer cells and vector controls had a similar growth curve (Fig. 1*d*).

To investigate the potential effect of PTHrP on tumorigenicity, male athymic mice were injected subcutaneously in each flank with $5 \times 10^4$ tumor cells. Subcutaneous tumors were dissected and weighed after 6 weeks. As shown in Figures 1*e* and 1*f*, PTHrP overexpressing cells resulted in larger tumors than vector control ($0.34 \pm 0.16$ g *vs.* $0.08 \pm 0.04$ g, $p < 0.01$). Histology demonstrated no qualitative difference in vascularization, as determined by vWF immunohistostaining, in PTHrP-overexpressing tumors and vector control tumors (Fig. 1*g*). Ki-67 immunohistostaining of PTHrP-overexpressing tumors demonstrated PTHrP increased cell proliferation (Fig. 1*h*; PTHrP 11% ± 1.2% *vs.* control 6.9% ± 0.8%, $p < 0.05$).

### *Impact of prostate cancer-derived PTHrP on bone*

To investigate the effects of tumor-derived PTHrP on bone during skeletal progression, prostate cancer clones with PTHrP overexpression or vector controls were co-implanted with donor vertebrae. After 6 weeks, implants were removed from transplant recipients and radiographed. PTHrP-overexpressing clones resulted in radiographically denser bone implants (Fig. 2*a*). Trichrome staining of implant sections further demonstrated increased total bone area ($0.36 \pm 0.22$ mm$^2$ *vs.* $0.12 \pm 0.06$ mm$^2$, $p < 0.001$) (Figs. 2*b* and 2*c*) in PTHrP-overexpressing implants. PTHrP-overexpressing implants also had larger tumors (Fig. 2*d*), while the index of bone area/tumor area was still significantly greater than the vector control group (Fig. 2*e*).

### *Alteration of microenvironment by PTHrP overexpressing prostate cancer cells*

The morphology of tumors in vossicles with H&E staining is shown in Figure 3. Compared to the vector control group, PTHrP overexpression resulted in significantly more osteoclasts ($3.32 \pm 1.34$ mm *vs.* $0.78 \pm 0.64$ mm, $p < 0.001$) (Fig. 3*c*). The PTHrP group also had more osteoclast-covered bone surface perimeter than vector control (7.73% ± 3.25% *vs.* 2.23% ± 1.90%, $p < 0.001$) (Fig. 3*d*). PTHrP immunohistochemistry showed that PTHrP-overexpressing tumor microfoci expressed high levels of PTHrP adjacent to osteoblastic lesions (Fig. 3*g*) and large islands of bone, as shown in H&E and Trichome stain, formed around microtumor foci (Figs. 3*e* and 3*f*). A layer of blood vessels (as detected by vWF staining) was frequently seen around PTHrP-expressing tumors (Fig. 3*h*). In H&E staining, mesenchymal cells surrounded tumors and filled the space between tumors and bones (Figs. 3*b* and 3*e*). Blood vessels localized at the interface between tumor and mesenchymal cells. The microvessel density (MVD) in PTHrP overexpressing implants was significantly greater compared to the vector controls ($18.5 \pm 2.69$ *vs.* $7.1 \pm 0.75$) (Fig. 3*k*).

### *PTHrP over-expressing prostate cancer enhanced osteoblastogenesis*

Bone marrow stromal cell populations contain osteoblast precursors. To determine the effect of PTHrP on osteoblast commitment, bone marrow cells from long bones (tibia and femur) were

plated and treated with various concentrations of PTHrP (1–34) or vehicle every other day for 10 days, and ALP-positive and total colony forming units were compared. The number of CFU-ALP were increased by PTHrP at concentrations of 10–100 nM, while the relative CFU-F were unchanged at these concentrations (Figs. 4*a* and 4*b*). The pro-proliferative effect of PTHrP on early stage osteoblasts has been reported.[36] Consistently, PTHrP treatment enhanced the numbers of BMSC during a 6-day period (Fig. 4*c*). To evaluate osteoblastogenesis of tumor-derived PTHrP, BMSC were co-cultured with either vector control or PTHrP-overexpressing prostate cancer cells. PTHrP-overexpressing prostate cancer caused increased ALP staining compared to vector control (4.5 ± 0.2 *vs*. 2.6 ± 0.1 arbitrary units, PTHrP overexpressing *vs*. vector control, $p < 0.001$) (Figs. 4*d* and 4*e*). These results were compared to the effects seen with treatment of BMSC cultures with vehicle or 10 nM PTHrP (1–34) (1.0 ± 0.1 *vs*. 3.6 ± 0.6 arbitrary units, $p < 0.001$). All the tested PTHrP-overexpressing clones induced increased ALP staining compared to the vector control (Fig. 4*f*).

*PTHrP enhanced osteoclastogenesis* ex vivo

The effect of PTHrP on osteoclastogenesis was determined by treating whole bone marrow in culture every other day for 10 days, followed by TRAP staining and enumeration of multinucleated TRAP positive cells. The number of TRAP-positive, multinucleated osteoclasts was increased with PTHrP treatment in a dose-dependent manner (Figs. 5*a* and 5*b*). PTHrP also enhanced the numbers of nuclei per TRAP-positive cell (Fig. 5*c*). All the tested PTHrP-overexpressing clones induced increased osteoclastogenesis compared to the vector control (Fig. 5*d*).

*Increased microvessels in human prostate cancer metastasis*

Immunostaining of vWF in a human prostate cancer tissue array demonstrated that skeletal metastases had increased microvessel density (MVD), compared to that of normal prostate and primary prostate cancer (Figs. 6*a* and 6*b*). Immunolocalization in human prostate cancer autopsy revealed that vWF positivity was adjacent to the area of PTHrP immunostaining in prostate cancer skeletal metastases (Fig. 6*c*).

*PTHrP enhanced angiogenesis indirectly via BMSCs*

Though it was reported that endothelial cells have low levels of PTHR1 detected by reverse transcription and PCR, it has not been reported to be detected using other approaches.[37] Endothelial cells also lack PTHrP binding activity as measured with $^{125}$I-labeled PTHrP.[38] Using highly sensitive and specific real-time PCR, PTHR1 expression in HAEC and HBME endothelial cells was tested in this study using human osteosarcoma SaOS cell line as the positive control. The PTHR1 was not detectable in the endothelial cell lines (Fig. 7*a*).

The histology of PTHrP overexpressing prostate cancer-induced osteoblastic lesions identified regions of angiogenesis localized at the interface of PTHrP-expressing tumor and mesenchymal cells (Fig. 3*h*). These findings suggested that PTHrP may act indirectly to promote angiogenesis. To test this hypothesis, *in vitro* angiogenesis assays were evaluated using human aortic endothelial cells. Endothelial cells were treated with PTHrP in the presence or absence of BMSC. Neither PTHrP nor BMSC alone caused the formation of vascular sprouts (Figs. 7*b*–7*d*). In contrast, PTHrP in the presence of BMSC significantly enhanced vascular sprouts. To evaluate the pro-angiogenic effect of tumor-derived PTHrP, endothelial cells were co-cultured with either vector control or PTHrP overexpressing prostate cancer cells in the presence or absence of BMSC. Compared to no tumor cells, vector control tumor cells alone increased vascular sprouts in either the presence or absence of BMSC, suggesting angiogenic factors are produced by prostate cancer cells. In the absence of bone marrow cells, PTHrP overexpression did not alter vascular sprouts as compared to vector controls. In the presence of BMSC, PTHrP-overexpressing cells

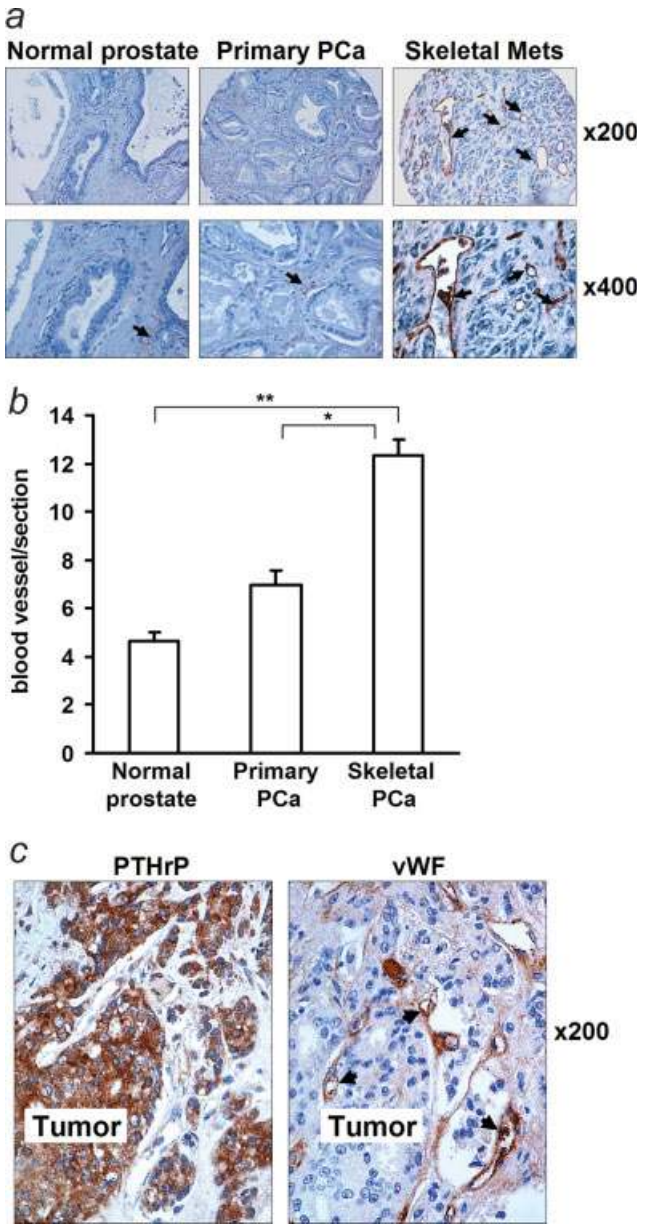


**Figure 6** – MVD in human autopsy specimens. (*a*) Representative images of vWF staining in human PCa tissue array. Blood vessels are indicated with arrows; (*b*) total number of blood vessels were counted per section of tissue array (*$p < 0.05$, **$p < 0.01$); (*c*) immunohistostaining for PTHrP and vWF in human prostate cancer skeletal metastatic lesions. Blood vessels are indicated with arrows.

resulted in a much higher level of vascular sprouting. Since coculture of endothelial cells with BMSC did not result in formation of vascular sprouting (Figs. 7*b* and 7*d*), this suggested that BMSC are mediators of vascular sprouting induced by PTHrP overexpressing tumor cells.

To identify potential factors induced by PTHrP in BMSC, several angiogenic cytokines were measured using real-time PCR (Figs. 8*a*–8*d*). The production of IL-6 and CXCL1 by BMSC were rapidly and significantly induced by PTHrP. At 1 hr, the mRNA level of IL-6 increased more than 180-fold and CXCL1 increased more than 60-fold. PTHrP also induced a moderate increase of MCP-1 (6.7-fold at 4 hr) and a less but still significant increase in VEGF (1.3-fold at 1 hr). To confirm that the increase in vascular sprouting by PTHrP-overexpressing tumors was due to PTHrP,

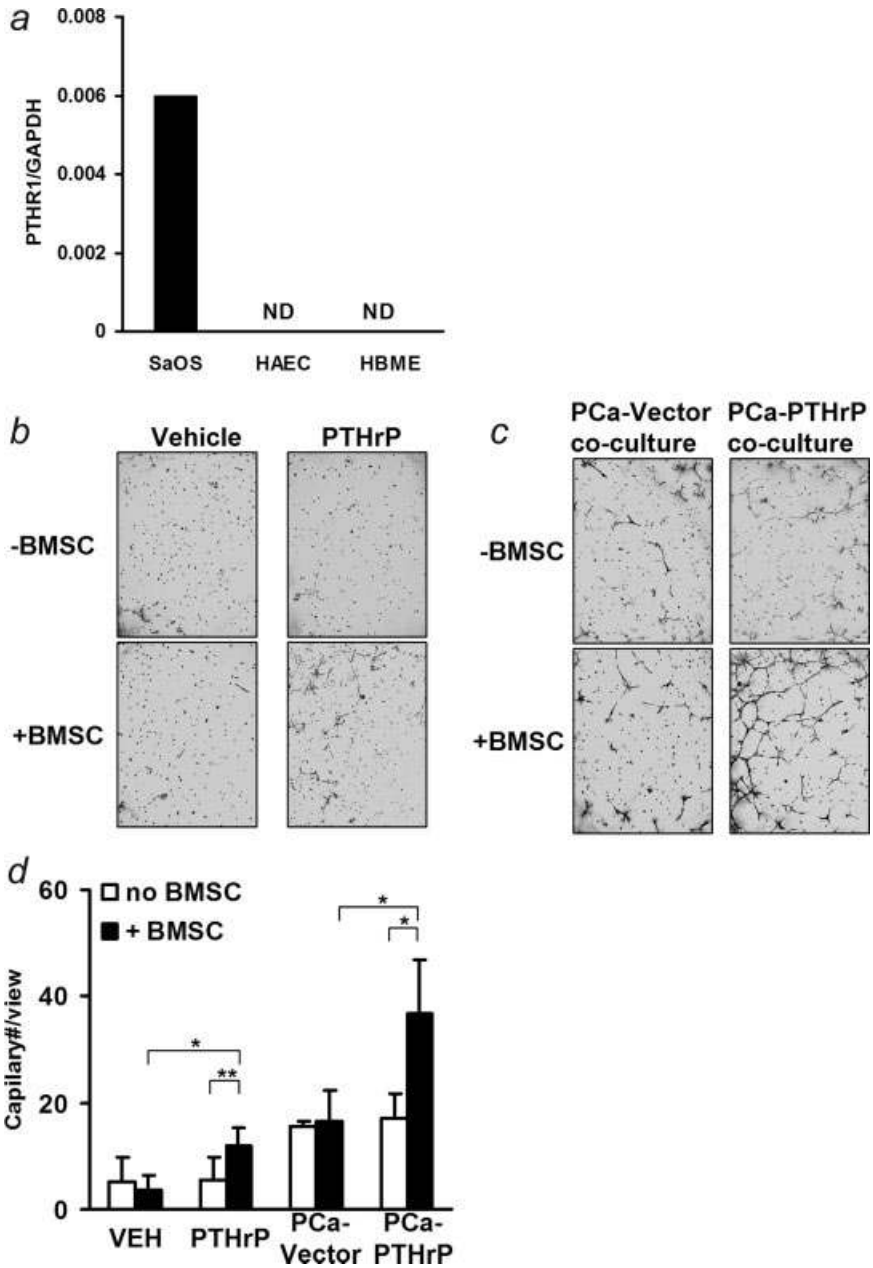


**Figure 7** – PTHrP induced angiogenesis with bone marrow stromal cells. (*a*) Detection of PTHR1 in endothelial cells with reverse transcription and real-time PCR (ND, not detectable); (*b*) representative data of *in vitro* angiogenesis analysis in response to vehicle or PTHrP (10 nM) treatment in the presence (+BMSC) or absence of bone marrow stromal cells(−BMSC); (*c*) representative data of *in vitro* angiogenesis analysis in the presence (+BMSC) or absence of bone marrow stromal cells(-BMSC) when co-cultured with prostate cancer cells (magnification ×40); (*d*) quantitative data of *in vitro* angiogenesis analysis (*$p < 0.05$, **$p < 0.01$, $n = 4$–6).

PTHrP (7–34) was used as an antagonist to suppress PTHrP signaling. PTHrP(7–34) prevents PTHrP binding to its receptor and blocks its signaling.[39] Two micromolar PTHrP(7–34) was chosen to give sufficient and sustained suppression for PTHrP signaling during the *in vitro* vascular sprouting assay. PTHrP(7–34) was able to suppress the increase in vascular sprouting induced by PTHrP-overexpressing tumor cells (Fig. 8*e*).

## Discussion

Expression of PTHrP correlates with the progression of skeletal metastasis in prostate cancer patients.[40] Substantial *in vivo* studies support that PTHrP expression regulates tumor progression.[15,41–43] One possible mechanism for this effect is that PTHrP enhances bone turnover and releases bioactive factors that facilitate tumor localization and growth in bone.[2,6–11] In this study, the effects of PTHrP on tumorigenesis and cancer-induced bone lesions were investigated with a mouse model using canine prostate cancer cells that were stably transfected to overexpress full length PTHrP.

ACE-1 is a canine prostate cancer cell line that is particularly useful in these studies because of its ability to induce osteoblastic lesions similar to those often seen in human prostate cancer.[28] Radiographs of tumors generated by these cells demonstrate a mixed osteoblastic/osteolytic lesion. The ACE-1 cells express low levels of endogenous PTHrP, and no detectable PTHR1 (supplementary

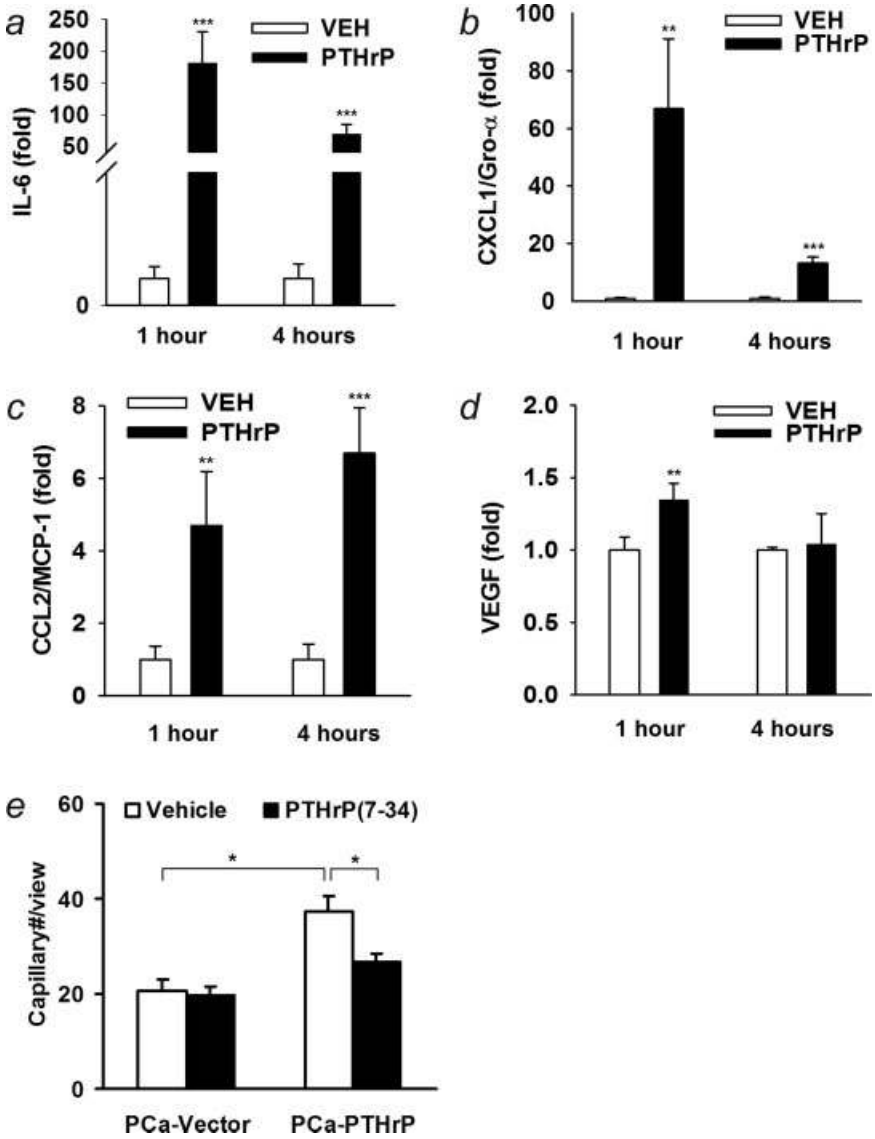


**Figure 8** – Bone marrow stromal cells were challenged with 10 nM PTHrP. (*a–d*) The mRNA levels of pro-angiogenic factors, IL-6, CXCL1, MCP-1 and VEGF were measured using reverse transcription and real-time PCR (**$p < 0.01$, ***$p < 0.001$, PTHrP *vs.* vehicle, $n = 4$); (*e*) HAEC *in vitro* angiogenesis analysis when co-cultured with prostate cancer cells and BMSC. PTHrP(7–34) (2 μM) suppressed PTHrP-overexpressing PCa induced increase in vascular sprouting (*$p < 0.05$, $n = 4$).

data). ACE-1 cells express a number of cytokines, such as VEGF, FGF-2 and PDGF-BB.[44] Transfection of full length rat PTHrP DNA resulted in upregulation of PTHrP levels. ACE-1 cells with high levels of PTHrP demonstrated increased tumorigenicity after subcutaneous inoculation into athymic mice, as determined by increased tumor weight in PTHrP transfectants *vs*. vector controls. Consistently, ACE-1 cells with increased PTHrP expression grew more rapidly *in vitro*. This could be associated with the antiapoptotic activity of the nuclear localization sequence (amino-acid 87–107) that we have previously described.[29]

A typical osteoblastic histological pattern was observed in vertebrae implants with PTHrP-overexpressing tumors, in which new bone was formed around microtumor foci, with increased adjacent osteoblasts and osteoclasts. Increased numbers of osteoclasts in implants with PTHrP-overexpressing tumors suggested increased bone turnover caused by PTHrP. Mesenchymal cells surrounded tumors and filled the space between tumors and bones. Interestingly, a layer of blood vessels (as detected by vWF staining) was frequently seen at the interface between tumor and mesenchymal cells. These data suggest that tumor-derived PTHrP is actively involved in the processes of osteoblastogenesis, osteoclastogenesis and angiogenesis, which would imply that PTHrP is an important factor responsible for pathological alterations of prostate cancer-induced bone lesions.

Osteoblasts and osteoclasts are 2 major cell mediators of bone remodeling. PTH/PTHrP supports osteoclastogenesis by upregulating RANKL and MCP-1 in osteoblasts.[22,23] Consistent in this study, PTHrP enhanced osteoclast formation *in vitro* from bone marrow cells in a concentration-dependent manner, correlating with the *in vivo* results showing increased osteoclastogenesis with increased PTHrP expression.

Prostate cancer-derived PTHrP is also a stimulator of osteoblastogenesis. In this study, BMSC in culture exhibited increased proliferation when treated with PTHrP as compared to controls. BMSC are precursors of several cell types including osteoblasts.[45] Previous studies have shown that cyclin D1 is a key target of PTHrP that mediates PTHrP-induced proliferation in early osteoblastic cells.[36] When co-cultured with BMSC, PTHrP-overex-

pressing prostate cancer cells stimulated ALP staining, suggesting development of early osteoblastic cells. The *in vitro* proliferation and osteoblast commitment assays supported the hypothesis that PTHrP enhanced osteoblastogenesis by stimulating osteoblast progenitor cell proliferation and by inducing early osteoblast differentiation.

The successful establishment of metastasis relies on vascularization.[46] New blood vessels are initially formed through the assembly or sprouting of endothelial cells. The recruitment of supporting pericytes and vascular smooth muscle cells ensures the formation of a mature and stable vascular network.[47] Within the vasculature, endothelial cells produce PTHrP, while the PTH/PTHrP receptor is reported to be located in pericytes and smooth muscle cells.[48] PTHrP produced by endothelial cells acts on smooth muscle cells and may be of importance for the growth and development of new vasculature.[38] Interestingly, there are contradictory reports about the effects of PTHrP on angiogenesis.[49–52] An inhibitory effect on angiogenesis was first reported in an *in vivo* model with the chick chorioallantoic membrane.[49] PTHrP gene delivery by adenovirus also inhibited angiogenesis and growth of subcutaneous prostate tumors.[49] Some reports have suggested that PTHrP may inhibit angiogenesis by suppressing endothelial migration in a protein kinase A-dependent manner.[49] In fetal skin of PTHrP or PTHR1 knockout mice, increases in the length, diameter and density of capillaries were observed.[50] In contrast, rat pituitary malignant tumor cells, mGH3, which overexpressed PTHrP, exhibited hypervascularization in xenografts *in vivo*.[51] Co-incubation with antisense PTHrP oligonucleotide (10 μM), but not sense or mismatched PTHrP oligonucleotide, suppressed mGH3-induced hypervascularization in diffusion chambers.[51] In a breast adenocarcinoma cell line (MDA-231), PTHrP enhanced the production of connective tissue growth factor (CTGF/CCN2), a factor that regulates endothelial proliferation and migration, by autocrine or paracrine mechanisms.[52] Since PTHR1 is absent on endothelial cells, contradictory observations may result from the difference in environment where different PTHrP targeted cells exist.

This study showed that there was no significant difference in density of vascularity between subcutaneous PTHrP-overexpressing tumors and vector control tumors. However, increased angiogenesis was observed in vossicles co-implanted with PTHrP-overexpressing prostate cancer cells compared to vossicles co-implanted with vector control, indicating that the pro-angiogenic effect of PTHrP may require the unique bone microenvironment. Noticeably, an increase in angiogenesis was found at the interface of PTHrP overexpressing prostate cancer microfoci and mesenchymal cells in vossicle implants. Thus, it is likely that tumor-derived PTHrP may exert its proangiogenic effect indirectly via BMSC.

To test this, an *in vitro* assay was performed to examine involvement of BMSCs in the pro-angiogenic effect of PTHrP. The results showed that endothelial cells barely formed vascular sprouts, in the presence of either PTHrP or BMSC. In the presence of both PTHrP and BMSC, a significant increase in endothelial cell-mediated angiogenesis was observed. These data support the hypothesis that PTHrP acts as a pro-angiogenic factor via BMSCs. Co-culture of endothelial cells with either vector control, or PTHrP-overexpressing prostate cancer cells resulted in similar levels of angiogenesis. In contrast, in the presence of BMSC, PTHrP overexpressing transfectants caused significantly higher angiogenesis than vector control. The data support that tumor-derived PTHrP enhances angiogenesis via BMSC. Upon examination, the induction of several angiogenic factors including IL-6, CXCL1, MCP-1 and VEGF from BMSC with PTHrP treatment was found. Suppression of PTHrP overexpressing cancer cell-induced vascular sprouting by PTHrP (7–34) supported PTHrP as the key mediator. Using human clinical autopsy specimens, this study also demonstrated prostate cancer skeletal metastases have abundant vasculature compared to primary tumors. In human autopsy specimens, microvessels aligned along the surface of PTHrP expressing microfoci. The data suggest prostate cancer-derived PTHrP is a pro-angiogenic agent in skeletal metastasis by mediating the interactions between tumor and bone microenvironment.

Expression of PTHrP has been identified in many cancers, such as prostate, breast, lung and others. Breast cancer-derived PTHrP is an important factor associated with osteolytic lesions via enhancing osteoclastogenesis.[1–3] Unlike breast cancer, most prostate cancers result in osteoblastic skeletal lesions.[3] Prostate cancer produces several osteoblastic factors, such as BMPs, TGF-β, FGFs, IGFs, PDGF, VEGF and endothelins.[25] This study demonstrated that prostate cancer-derived PTHrP enhances both osteoclastogenesis and osteoblastogenesis. PTHrP, therefore, may prime bone remodeling and mediate prostate cancer-induced osteoblastic lesions. This study also provides evidence that PTHrP is a mediator of tumor-associated angiogenesis. PTHrP exerted its pro-angiogenic effect via BMSC by stimulating the production of a number of angiogenic factors in these cells. Since angiogenesis not only facilitates the establishment of metastasis, but is also an important early step for bone formation,[26,53] PTHrP is a key mediator of prostate cancer skeletal progression. Targeting factors, such as PTHrP, that mediate prostate cancer-bone microenvironment interactions will be a promising strategy for therapy and prevention of prostate cancer skeletal progression.

## Acknowledgements

We thank Mr. Chris Strayhorn (University of Michigan, School of Dentistry Histology Core Facility) for technical assistance with histological preparation of samples; and Drs. Russell Taichman, Jianhua Wang and Jason Wang for assistance with immunohistochemistry and *in vitro* angiogenesis analysis.

## References

1. Coleman RE. Skeletal complications of malignancy. Cancer 1997; 80:1588–94.
2. Roodman GD. Mechanisms of bone metastasis. N Engl J Med 2004;350:1655–64.
3. Mundy GR. Metastasis to bone: causes, consequences and therapeutic opportunities. Nat Rev Cancer 2002;2:584–93.
4. Imbriaco M, Larson SM, Yeung HW, Mawlawi OR, Erdi Y, Venkatraman ES, Scher HI. A new parameter for measuring metastatic bone involvement by prostate cancer: the bone scan index. Clin Cancer Res 1998;4:1765–72.
5. Roudier MP, True LD, Higano CS, Vesselle H, Ellis W, Lange P, Vessella RL. Phenotypic heterogeneity of end-stage prostate carcinoma metastatic to bone. Hum Pathol 2003;34:646–53.
6. Schneider A, Kalikin LM, Mattos AC, Keller ET, Allen MJ, Pienta KJ, McCauley LK. Bone turnover mediates preferential localization of prostate cancer in the skeleton. Endocrinology 2005;146:1727–36.
7. Miwa S, Mizokami A, Keller ET, Taichman R, Zhang J, Namiki M. The bisphosphonate YM529 inhibits osteolytic and osteoblastic changes and CXCR-4-induced invasion in prostate cancer. Cancer Res 2005;65:8818–25.
8. Clezardin P, Ebetina FH, Fournier PG. Bisphosphonates and cancer-induced bone disease: beyond their antiresorptive activity. Cancer Res 2005;65:4971–4.
9. Smith MR. Zoledronic acid to prevent skeletal complications in cancer: corroborating the evidence. Cancer Treat Rev 2005;31 (Suppl 3): 19–25.
10. Michaelson MD, Smith MR. Bisphosphonates for treatment and prevention of bone metastases. J Clin Oncol 2005;23:8219–24.
11. Liao J, Schneider A, Datta NS, McCauley LK. Extracellular calcium as a candidate mediator of prostate cancer skeletal metastasis. Cancer Res 2006;66:9065–73.
12. Adams GB, Chabner KT, Alley IR, Olson DP, Szczepiorkowski ZM, Poznansky MC, Kos CH, Pollak MR, Brown EM, Scadden DT. Stem cell engraftment at the endosteal niche is specified by the calcium-sensing receptor. Nature 2006;439:599–603.
13. Sanders JL, Chattopadhyay N, Kifor O, Yamaguchi T, Butters RR, Brown EM. Extracellular calcium-sensing receptor expression and its potential role in regulating parathyroid hormone-related peptide secretion in human breast cancer cell lines. Endocrinology 2000;141:4357–64.

14. Liao J, McCauley LK. Skeletal metastasis: established and emerging roles of parathyroid hormone related protein (PTHrP). Cancer Metastasis Rev 2006;25:559–71.
15. Deftos LJ, Barken I, Burton DW, Hoffman RM, Geller J. Direct evidence that PTHrP expression promotes prostate cancer progression in bone. Biochem Biophys Res Commun 2005;327:468–72.
16. Hoey RP, Sanderson C, Iddon J, Brady G, Bundred NJ, Anderson NG. The parathyroid hormone-related protein receptor is expressed in breast cancer bone metastases and promotes autocrine proliferation in breast carcinoma cells. Br J Cancer 2003;88:567–73.
17. Cataisson C, Lieberherr M, Cros M, Gauville C, Graulet AM, Cotton J, Calvo F, de Vernejoul MC, Foley J, Bouizar Z. Parathyroid hormone-related peptide stimulates proliferation of highly tumorigenic human SV40-immortalized breast epithelial cells. J Bone Miner Res 2000;15:2129–39.
18. Massfelder T, Lang H, Schordan E, Lindner V, Rothhut S, Welsch S, Simon-Assmann P, Barthelmebs M, Jacqmin D, Helwig JJ. Parathyroid hormone-related protein is an essential growth factor for human clear cell renal carcinoma and a target for the von Hippel-Lindau tumor suppressor gene. Cancer Res 2004;64:180–8.
19. Shen X, Falzon M. PTH-related protein enhances LoVo colon cancer cell proliferation, adhesion, and integrin expression. Regul Pept 2005; 125:17–27.
20. Shen X, Falzon M. PTH-related protein modulates PC-3 prostate cancer cell adhesion and integrin subunit profile. Mol Cell Endocrinol 2003;199:165–77.
21. Hastings RH, Araiza F, Burton DW, Zhang L, Bedley M, Deftos LJ. Parathyroid hormone-related protein ameliorates death receptor-mediated apoptosis in lung cancer cells. Am J Physiol Cell Physiol 2003; 285:C1429–C1436.
22. Ma YL, Cain RL, Halladay DL, Yang X, Zeng Q, Miles RR, Chandrasekhar S, Martin TJ, Onyia JE. Catabolic effects of continuous human PTH (1–38) in vivo is associated with sustained stimulation of RANKL and inhibition of osteoprotegerin and gene-associated bone formation. Endocrinology 2001;142:4047–54.
23. Li X, Qin L, Bergenstock M, Bevelock LM, Novack DV, Partridge NC. Parathyroid hormone stimulates osteoblastic expression of MCP-1 to recruit and increase the fusion of pre/osteoclasts. J Biol Chem 2007;282:33098–106.
24. Martin TJ, Quinn JM, Gillespie MT, Ng KW, Karsdal MA, Sims NA. Mechanisms involved in skeletal anabolic therapies. Ann N Y Acad Sci 2006;1068:458–70.
25. Logothetis CJ, Lin SH. Osteoblasts in prostate cancer metastasis to bone. Nat Rev Cancer 2005;5:21–8.
26. Gerber HP, Vu TH, Ryan AM, Kowalski J, Werb Z, Ferrara N. VEGF couples hypertrophic cartilage remodeling, ossification and angiogenesis during endochondral bone formation. Nat Med 1999;5:623–8.
27. Hall CL, Bafico A, Dai J, Aaronson SA, Keller ET. Prostate cancer cells promote osteoblastic bone metastases through Wnts. Cancer Res 2005;65:7554–60.
28. LeRoy BE, Thudi NK, Nadella MV, Toribio RE, Tannehill-Gregg SH, van Bokhoven A, Davis D, Corn S, Rosol TJ. New bone formation and osteolysis by a metastatic, highly invasive canine prostate carcinoma xenograft. Prostate 2006;66:1213–22.
29. Dougherty KM, Blomme EA, Koh AJ, Henderson JE, Pienta KJ, Rosol TJ, McCauley LK. Parathyroid hormone-related protein as a growth regulator of prostate carcinoma. Cancer Res 1999;59:6015–22.
30. Bernardi R, Guernah I, Jin D, Grisendi S, Alimonti A, Teruya-Feldstein J, Cordon-Cardo C, Simon MC, Rafii S, Pandolfi PP. PML inhibits HIF-1alpha translation and neoangiogenesis through repression of mTOR. Nature 2006;442:779–85.
31. Koh AJ, Demiralp B, Neiva KG, Hooten J, Nohutcu RM, Shim H, Datta NS, Taichman RS, McCauley LK. Cells of the osteoclast lineage as mediators of the anabolic actions of parathyroid hormone in bone. Endocrinology 2005;146:4584–96.
32. Yang F, Tuxhorn JA, Ressler SJ, McAlhany SJ, Dang TD, Rowley DR. Stromal expression of connective tissue growth factor promotes angiogenesis and prostate cancer tumorigenesis. Cancer Res 2005; 65:8887–95.
33. Pettway GJ, Schneider A, Koh AJ, Widjaja E, Morris MD, Meganck JA, Goldstein SA, McCauley LK. Anabolic actions of PTH (1–34): use of a novel tissue engineering model to investigate temporal effects on bone. Bone 2005;36:959–70.
34. Chen TL. Inhibition of growth and differentiation of osteoprogenitors in mouse bone marrow stromal cell cultures by increased donor age and glucocorticoid treatment. Bone 2004;35:83–95.
35. Zeng Q, Li S, Chepeha DB, Giordano TJ, Li J, Zhang H, Polverini PJ, Nor J, Kitajewski J, Wang CY. Crosstalk between tumor and endothelial cells promotes tumor angiogenesis by MAPK activation of Notch signaling. Cancer Cell 2005;8:13–23.
36. Datta NS, Pettway GJ, Chen C, Koh AJ, McCauley LK. Cyclin D1 as a target for the proliferative effects of PTH and PTHrP in early osteoblastic cells. J Bone Miner Res 2007;22:951–64.
37. Isales CM, Sumpio B, Bollag RJ, Zhong Q, Ding KH, Du W, Rodriguez-Commes J, Lopez R, Rosales OR, Gasalla-Herraiz J, McCarthy R, Barrett PQ. Functional parathyroid hormone receptors are present in an umbilical vein endothelial cell line. Am J Physiol Endocrinol Metab 2000;279:E654–E662.
38. Rian E, Jemtland R, Olstad OK, Endresen MJ, Grasser WA, Thiede MA, Henriksen T, Bucht E, Gautvik KM. Parathyroid hormone-related protein is produced by cultured endothelial cells: a possible role in angiogenesis. Biochem Biophys Res Commun 1994;198:740–7.
39. McKee RL, Goldman ME, Caulfield MP, DeHaven PA, Levy JJ, Nutt RF, Rosenblatt M. The 7–34-fragment of human hypercalcemia factor is a partial agonist/antagonist for parathyroid hormone-stimulated cAMP production. Endocrinology 1988;122:3008–10.
40. Bryden AA, Hoyland JA, Freemont AJ, Clarke NW, George NJ. Parathyroid hormone related peptide and receptor expression in paired primary prostate cancer and bone metastases. Br J Cancer 2002;86:322–325.
41. Iguchi H, Tanaka S, Ozawa Y, Kashiwakuma T, Kimura T, Hiraga T, Ozawa H, Kono A. An experimental model of bone metastasis by human lung cancer cells: the role of parathyroid hormone-related protein in bone metastasis. Cancer Res 1996;56:4040–3.
42. Guise TA, Yin JJ, Taylor SD, Kumagai Y, Dallas M, Boyce BF, Yoneda T, Mundy GR. Evidence for a causal role of parathyroid hormone-related protein in the pathogenesis of human breast cancer-mediated osteolysis. J Clin Invest 1996;98:1544–9.
43. Guise TA, Yin JJ, Thomas RJ, Dallas M, Cui Y, Gillespie MT. Parathyroid hormone-related protein (PTHrP)-(1–139) isoform is efficiently secreted *in vitro* and enhances breast cancer metastasis to bone *in vivo*. Bone 2002;30:670–6.
44. Thudi NK, Nadella PMV, Rosol TJ. Modulation of osteoblastic activity by the canine prostate cancer cells. Skeletal complications of malignancy V (meeting abstract) p 90, 2007.
45. Aubin JE, Liu F, Malaval L, Gupta AK. Osteoblast and chondroblast differentiation. Bone 1995;17:77S–83S.
46. Zetter BR. Angiogenesis and tumor metastasis. Ann Rev Med 1998; 49:407–24.
47. Foo SS, Turner CJ, Adams S, Compagni A, Aubyn D, Kogata N, Lindblom P, Shani M, Zicha D, Adams RH. Ephrin-B2 controls cell motility and adhesion during blood-vessel-wall assembly. Cell 2006; 124:161–73.
48. Funk JL, Wei H, Downey KJ, Yocum D, Benjamin JB, Carley W. Expression of PTHrP and its cognate receptor in the rheumatoid synovial microcirculation. Biochem Biophys Res Commun 2002;297:890–7.
49. Bakre MM, Zhu Y, Yin H, Burton DW, Terkeltaub R, Deftos LJ, Varner JA. Parathyroid hormone-related peptide is a naturally occurring, protein kinase A-dependent angiogenesis inhibitor. Nat Med 2002;8: 995–1003.
50. Diamond AG, Gonterman RM, Anderson AL, Menon K, Offutt CD, Weaver CH, Philbrick WM, Foley J. Parathyroid hormone hormone-related protein and the PTH receptor regulate angiogenesis of the skin. J Invest Dermatol 2006;126:2127–34.
51. Akino K, Ohtsuru A, Kanda K, Yasuda A, Yamamoto T, Akino Y, Naito S, Kurokawa M, Iwahori N, Yamashita S. Parathyroid hormone-related peptide is a potent tumor angiogenic factor. Endocrinology 2000;141:4313–16.
52. Shimo T, Kubota S, Yoshioka N, Ibaragi S, Isowa S, Eguchi T, Sasaki A, Takigawa M. Pathogenic role of connective tissue growth factor (CTGF/CCN2) in osteolytic metastasis of breast cancer. J Bone Miner Res 2006;21:1045–59.
53. Wang Y, Wan C, Deng L, Liu X, Cao X, Gilbert SR, Bouxsein ML, Faugere MC, Guldberg RE, Gerstenfeld LC, Haase VH, Johnson RS, et al. The hypoxia-inducible factor alpha pathway couples angiogenesis to osteogenesis during skeletal development. J Clin Invest 2007; 117:1616–26.